ELEN E4830 Digital Image Processing

Homework 5 Solution

Chuxiang Li

cxli@ee.columbia.edu

Department of Electrical Engineering, Columbia University

March 27, 2006

1 Motion Blur Filter

Coordinate Transform: Rectangular Coordinate $\Longrightarrow$ Polar Coordinate

First, we convert the image from rectangular coordinate to polar coordinate. In particular, for any pixel with rectangular coordinate $(x; y)$, the corresponding pixel with polar coordinate is $(r; \theta)$ where

$$\begin{cases} r = \sqrt{x^2 + y^2}, \\ \theta = \tan^{-1}\left(\frac{y}{x}\right). \end{cases} \tag{1}$$

Model of Motion Blur in Polar Coordinate

After the coordinate transform operation (1), the blurring will then appear as one dimensional uniform motion blur along the θ-axis. Specifically, let T be the duration of exposure, $f(r, \theta)$ be the original image and $f(r - r_0(t), \theta - \theta_0(t))$ be the blurred image at each time

instant t in polar coordinate. When ignoring the noise, we have the following observation of the motion-blurred image

$$g(r,\theta) = \int_0^T f(r - r_0(t), \theta - \theta_0(t))dt, \tag{2}$$

where $r_0(t)$ and $\theta_0(t)$ denote the time-varying components of motion along r-axis and θ-axis, respectively. Taking Fourier transform of (2), we get the blurred image in Fourier domain

$$\begin{aligned}
G(w,\phi) &= \int_{-\infty}^{\infty}\int_0^{\infty} g(r,\theta)e^{-j2\pi(wr+\phi\theta)}drd\theta \\
&= \int_{-\infty}^{\infty}\int_0^{\infty}\left[\int_0^T f(r-r_0(t),\theta-\theta_0(t))dt\right]e^{-j2\pi(wr+\phi\theta)}drd\theta \\
&= \int_0^T \underbrace{\left[\int_{-\infty}^{\infty}\int_0^{\infty} f(r-r_0(t),\theta-\theta_0(t))e^{-j2\pi(wr+\phi\theta)}drd\theta\right]}_{\mathcal{F}\{f(r-r_0(t),\theta-\theta_0(t))\}=\mathcal{F}\{f(r,\theta)\}e^{-j2\pi[wr_0(t)+\phi\theta_0(t)]}} dt \\
&= \int_0^T F(w,\phi)e^{-j2\pi[wr_0(t)+\phi\theta_0(t)]}dt \\
&= F(w,\phi)\underbrace{\int_0^T e^{-j2\pi[wr_0(t)+\phi\theta_0(t)]}dt}_{H(w,\phi)},
\end{aligned} \tag{3}$$

where $\mathcal{F}\{f(r,\theta)\} = F(w,\phi)$ and $\mathcal{F}\{f(r-r_0(t),\theta-\theta_0(t))\}$ denote the Fourier transforms of the original image $f(r,\theta)$ and the blurred image $f(r-r_0(t),\theta-\theta_0(t))$, respectively; the fourth equality follows the property of Fourier transform; the fifth equality follows the fact that $F(w,\phi)$ is independent of time t. It should be noticed that θ is originally defined over $[0,2\pi]$ while here it is periodically extended to infinity.

It is observed that $H(w,\phi)$ in (3) denotes the Fourier transform of blurring along both r-axis and θ-axis. In this specific problem, we have

$$\begin{cases} r_0(t) = 0, \\ \theta_0(t) = \frac{\pi}{8T}t, \end{cases} \tag{4}$$

i.e., blurring only occurs along θ-axis. Then $H(w,\phi)$ in (3) can be further rewritten as

$$H(w,\phi) = \int_0^T e^{-j2\pi\phi\frac{\pi}{8T}t}dt = \frac{T}{\pi^2\phi/8}\sin(\pi^2\phi/8)e^{-j\pi^2\phi/8} = H(\phi). \tag{5}$$

Image Restoration for Motion Blurring and Noise in Polar Coordinate

Now the problem becomes the estimation of the original image $F(w,\phi)$ (i.e., $f(r,\theta)$), given $H(w,\phi)$ and the noisy observation

$$\tilde{G}(w,\phi) = F(w,\phi)\cdot H(w,\phi) + N(w,\phi),$$

where $N(w,\phi)$ is the noise in frequency domain. To solve this problem, several approaches can be employed to estimate $F(w,\phi)$ from $\tilde{G}(w,\phi)$. For instance,

$$\hat{F}_{\text{Inv}}(w,\phi) = \frac{\tilde{G}(w,\phi)}{H(w,\phi)} = F(w,\phi) + \frac{N(w,\phi)}{H(w,\phi)} \qquad \text{Inverse Filtering,} \tag{6}$$

$$\hat{F}_{\text{MMSE}}(w,\phi) = \left[\frac{|H(w,\phi)|^2}{H(w,\phi)[|H(w,\phi)|^2 + K]}\right]\tilde{G}(w,\phi) \qquad \text{MMSE (Wiener) Filtering.} \tag{7}$$

It is worth noting that in addition to (6) and (7), any approach dealing with uniform blur along one dimension can be applied here.

Coordinate Transform: Polar Coordinate $\Longrightarrow$ Rectangular Coordinate

After obtaining the estimate $\hat{F}(w,\phi)$ and thus the restored image $\hat{f}(r,\theta)$, we further convert $\hat{F}(w,\phi)$ ($\hat{f}(r,\theta)$) which falls in polar coordinate back to the corresponding $\hat{F}(u,v)$ ($\hat{f}(x,y)$) which falls in rectangular coordinate via the coordinate transform defined in (1).

Remark: In the solution above, we essentially treat this problem in the polar coordinate $(r;\theta)$ instead of the rectangular coordinate $(x;y)$. In particular, once obtaining (r,θ), we simply ignore the transform $(r;\theta)\Leftrightarrow(x;y)$, and treat (r,θ) as regular cartesian coordinates; after obtaining $\hat{F}(w,\phi)$ for (r,θ), we finally convert $\hat{F}(w,\phi)$ in (r,θ) back to $\hat{F}(u,v)$ in (x,y). The rationale behind the above approach is that it is extremely difficult to get the closed-form expression of $H(u,v)$ related to the rectangular coordinate $(x;y)$, because the non-linear property of the coordinate transform $(r;\theta)\Leftrightarrow(x;y)$ in (1) makes the problem intractable.

MB	AWGN	MB&AWGN	Inverse (MB)	ACF	NSR	Inverse
6.44dB	−2.82dB	−3.38dB	15.74dB	0.31dB	−1.37dB	−8.91dB

Table 1: SNR of different "Lena.jpg" images compared with the original image: "MB", "AWGN" and "MB&AWGN" correspond to the three contaminated images shown in Fig. 1; "Inverse (MB)" corresponds to the restored image from motion-blurring shown in Fig. 2; "ACF", "NSR" and "Inverse" correspond to the three restored images from motion-blurring and AWGN shown in Fig. 3.

2 Wiener Filtering

The original 3D-color image, "Lena.jpg", is shown in Fig. 1, where the motion-blurred version, the noisy version with additive white Gaussian noises (AWGN), and the corresponding image with both motion-blurring and AWGN are all shown. Fig. 2 shows the restoration image from the motion-blurred version. It is observed that with inverse filter, the restored "Lena.jpg" image has a very good quality compared with the original one. Fig. 3 shows the restoration effects of the "Lena.jpg" image with both motion-blurring and AWGN via three different restoration approaches. In particular, the results obtained using the Wiener filter with autocorrelation function (ACF), the Wiener filter with noise-to-signal ratio (NSR), and the inverse filter are all demonstrated. It is seen from Fig. 3 that the Wiener filter with ACF achieves the best performance, and the inverse filter has the worse performance.

Moreover, the objective performances, signal-to-noise ratio (SNR), of the "Lena.jpg" images in different conditions compared with the original version are all shown in Table 1. It is seen from Table 1 that the objective performances are consistent with the subjective performances shown in Fig. 1∼Fig. 3.

Figure 1: "Lena.jpg" in different conditions: the original image; the motion-blurred image; the noisy image with AWGN ($\sigma_n = 0.5$); the motion-blurred image with AWGN ($\sigma_n = 0.5$).

Figure 2: Restored "Lena.jpg" image from the motion-blurred version using inverse filter.

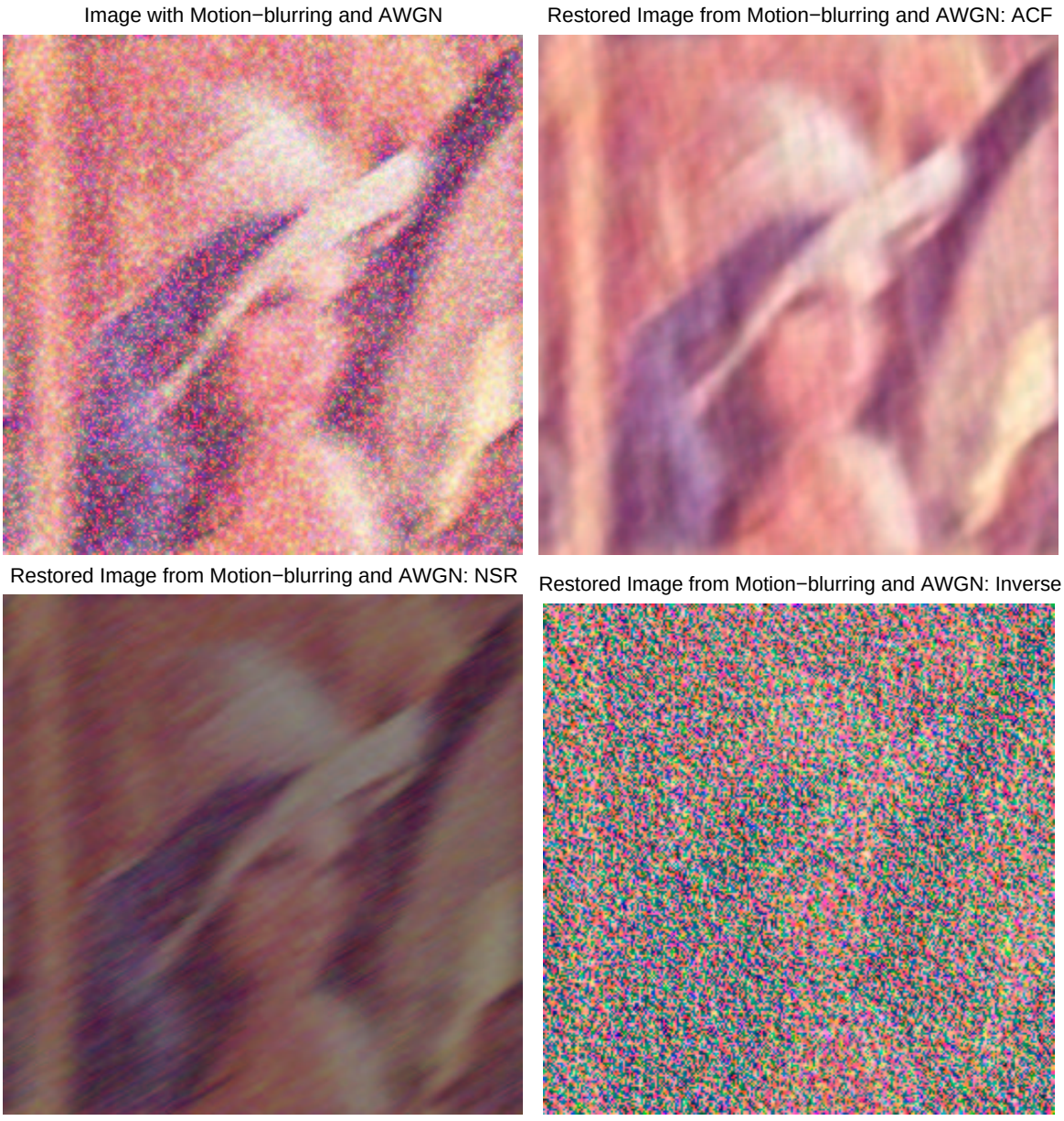

Figure 3: Restored "Lena.jpg" images from the image with both motion-blurring and AWGN: (1) ACF approach; (2) NSR approach; (3) inverse filter.